Chapter 26

Fluorescence and Reflectance Spectroscopy for Detection of Oral Dysplasia and Cancer

Richard A. Schwarz, Rebecca R. Richards-Kortum, and Ann M. Gillenwater

Introduction

Oral cancer is a serious health problem in many regions of the world. An estimated 263,000 new cases and 127,000 deaths due to oral cancer occur annually worldwide, including 24,000 new cases and 5500 deaths in the United States [1, 2]. The primary treatment method remains surgical resection, which may be followed by postoperative radiation therapy [3, 4]. Despite significant advances in treatment methods for oral cancer, patient survival rates have not shown substantial improvement. Failure to improve patient outcomes is likely secondary to delays in diagnosis until disease is at advanced stages, when treatment is more difficult, more morbid, and less successful than interventions for early oral cancers [5, 6]. Delayed diagnosis of patients with oral cancer is due in part to the lack of effective screening tools, insufficient education, difficulty in evaluating the risk of malignant transformation in oral potentially malignant lesions (OPMLs), and the high rate of recurrence following treatment [7–10].

The development and progression of neoplastic changes in the oral cavity lead to measurable changes in the optical properties of oral tissue. Malignant transformation results in alterations in metabolic activity and tissue architecture, that in turn cause changes in the natural autofluorescence of oral tissue derived from endogenous fluorophores in the epithelial and stromal layers [11, 12]. Microvascularization and reduced oxygen saturation cause

Brian J.-F. Wong and Justus Ilgner (eds.), Biomedical Optics in Otorhinolaryngology: Head and Neck Surgery,
DOI 10.1007/978-1-4939-1758-7_26, © Springer Science+Business Media New York 2016

changes in light absorption due to oxyhemoglobin and deoxyhemoglobin [13, 14]. Increased nuclear size, pleomorphism, and architectural changes alter the light scattering properties of tissue [15, 16].

These changes in optical properties during neoplastic progression can be detected using noninvasive optical techniques, potentially aiding in early detection and diagnosis. Observations of autofluorescence from tumor tissue in animals were reported as early as the 1920s [17]. Building on the extensive use of fluorescence to characterize cellular metabolism in the 1950s and 1960s [18, 19], optical spectroscopy emerged as a potential tool for clinical diagnostics in the 1980s [20, 21]. The rapid expansion of spectroscopic diagnostic methods at this time was facilitated by the availability of a wide variety of lasers for high-spectral intensity excitation and high-quality fiber optics for clinical probe development.

Various spectroscopic methods have been reported for the detection of dysplasia and cancer in the oral cavity and other organ sites, including fluorescence spectroscopy, elastic scattering spectroscopy, diffuse reflectance spectroscopy, Raman scattering spectroscopy, and time-resolved fluorescence spectroscopy, to name a few [22–24]. Each of these techniques involves the noninvasive interrogation of tissue using illumination light with selected characteristics and detection of the wavelength-dependent (spectral) characteristics of light emitted from the tissue to provide diagnostically relevant information. This chapter focuses on fluorescence spectroscopy, in which narrowband illumination light is used to excite endogenous fluorophores, and reflectance spectroscopy, in which broadband (white) illumination light is used to interrogate the elastic scattering properties and absorption properties of tissue.

Endogenous Fluorophores, Absorbers, and Scatterers in the Oral Mucosa

Light energy (photons) incident upon tissue can be absorbed by molecules naturally present within the tissue, either within cells or in the extracellular matrix. Certain types of these molecules can subsequently undergo a radiative relaxation process in which a photon with lower energy (longer wavelength) is emitted. This process is termed fluorescence. Autofluorescence refers to fluorescence from fluorophores naturally present in tissue. Sources of autofluorescence in oral tissue are shown in Table 1 [11]. These include the amino acids tryptophan, tyrosine, and phenylalanine; structural proteins including collagen, collagen crosslinks, and elastin; the coenzymes reduced nicotinamide adenine

Table 1

Endogenous tissue fluorophores

Fluorophore	Excitation maxima (nm)	Emission maxima (nm)
NADH	290,340	440,450
FAD	450	515
Collagen crosslinks	325	400
Elastin crosslinks	325	400
Collagen powder	280,265,330,450	310,385,390,530
Elastin powder	350,410,450	420,500,520
Tryptophan	280	350
Tyrosine	Not determined	300
Phenylalanine	Not determined	280
Pyridoxine	332	400
Lipofuscin	340–395	430–460,540
Eosinophils	370,500	440,550

NADH nicotinamide adenine dinucleotide, *FAD* flavine adenine dinucleotide, *nm* nanometers

Adapted with permission from Richards-Kortum R, Sevick-Muraca E. Ann Rev Phys Chem. 1996;47:555–606

dinucleotide (NADH) and flavin adenine dinucleotide (FAD); keratin; and porphyrins [25, 26]. The spatial distribution of these fluorophores is depth-dependent, with substantial differences between the epithelium and the supporting stroma [27]. Autofluorescence originating in the epithelium is primarily due to NADH, FAD, and a superficial keratin layer, which may be present depending on the anatomic site. In the stroma, collagen fibers, collagen crosslinks, and elastin fibers produce a strong fluorescence signal (Fig. 1).

Not all molecules that absorb light subsequently emit fluorescence. Hemoglobin, for example, undergoes a fast nonradiative relaxation and therefore does not exhibit measurable fluorescence except by highly specialized techniques; yet it is an important absorber of light in tissue [28, 29]. Oxy and deoxyhemoglobin have characteristic absorption spectra that may be readily observed in spectroscopic measurements of tissue using broadband illumination. The presence and relative concentration of oxy and deoxyhemoglobin may be detected through spectroscopic measurements.

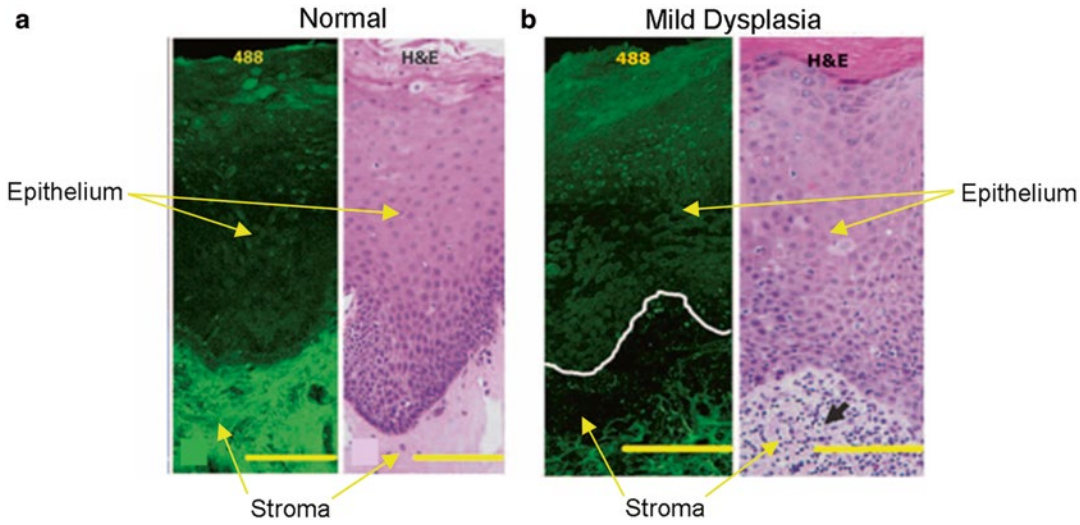

Fig. 1 Fluorescence confocal images of fresh oral tissue slices at 488 nm excitation, with corresponding hematoxylin and eosin (H&E) stained pathology sections. (**a**) Normal oral tissue without inflammation. (**b**) Oral tissue with mild dysplasia and mild/moderate inflammation, with the location of the basement membrane indicated by a *white line* in the confocal image. Note that the confocal images show intense stromal autofluorescence in (**a**) and reduced stromal autofluorescence in (**b**). Scale bars: 200 μm in the confocal images; 125 μm in the H&E images. *Black arrow*: lymphocytic infiltration. Adapted with permission from Pavlova I, Williams M, El-Naggar A, Richards-Kortum R, Gillenwater A. Clin Cancer Res. 2008;14(8):2396–2404

Tissue is a turbid medium in which light propagation is strongly affected by scattering as well as absorption. Photons that scatter elastically from cell nuclei, mitochondria, and other organelles undergo changes in propagation direction. Multiple scattering events may occur before a photon is absorbed or re-emitted from the tissue. Light scattering is sensitive to the size, shape, and distribution of the scatterers and is therefore affected by changes in nuclear/cytoplasm ratio and pleomorphism in cell nuclei.

With neoplastic progression the epithelium may display increased metabolic activity, increased nuclear size, increased nuclear/cytoplasm ratio, and pleomorphism, while the stroma may display enhanced microvascularization, influx of inflammatory cells, and breakdown of collagen crosslinks. Reduced blue-green stromal autofluorescence intensity and increased nuclear size and crowding within the epithelium are typically observed at dysplastic and cancerous sites. Thus spectroscopic measurements of tissue autofluorescence, absorption, and scattering may be used to characterize the disease state of tissue.

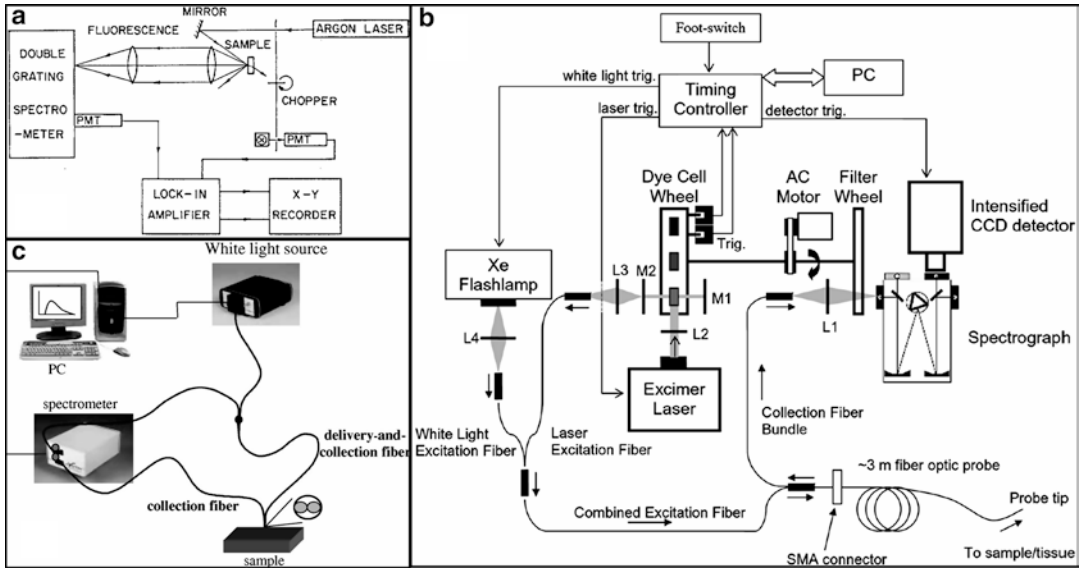

Fig. 2 Examples of spectroscopic instrumentation. (**a**) An early system used for laser-induced fluorescence spectroscopy of normal and cancerous animal tissue ex vivo. (**b**) A clinical system capable of laser-induced fluorescence spectroscopy at a range of excitation wavelengths, as well as reflectance spectroscopy. (**c**) A clinical system for differential path length reflectance spectroscopy. (**a**) Adapted with permission from Alfano RR, Tata DB, Cordero J, et al. *IEEE J Quant Electron*. 1984;QE-20(12):1507–1511. (**b**) Adapted with permission from Tunnell JW, Desjardins AE, Galindo L, et al. "Instrumentation for multi-modal spectroscopic diagnosis of epithelial dysplasia," *Technol Cancer Res Treat*. (http://www.tcrt.org), Adenine Press, 2003;2(6):505–514. (**c**) Adapted with permission from Amelink A, Kaspers OP, Sterenborg HJCM, et al. *Oral Oncol*. 2008;44:65–71

Instrumentation

The development of spectroscopic instrumentation for the detection of oral neoplasia over the past three decades has been driven primarily by technological advances in light sources, probes, spectrometers, and detectors; and secondarily by the demands of the clinical environment as these research devices have seen increasing clinical use. Figure 2a shows an early system used by Alfano et al. to perform laser-induced fluorescence spectroscopy of normal and cancerous animal tissue ex vivo [20]. The system included an argon laser source, a double grating spectrometer, photomultiplier tubes, and an x–y recorder. Advances in laser sources, fiber optics, and detectors soon led to the development of complex instruments capable of measuring a wide range of spectroscopic parameters in patients in vivo. Figure 2b shows a clinical spectroscopy system reported by Tunnell et al., capable of both laser-induced fluorescence spectroscopy at a range of excitation wavelengths (enabled by the tunable excimer-pumped dye laser) and

reflectance spectroscopy (enabled by the Xenon flashlamp) [30]. The system uses an intensified charge-coupled device (CCD) camera as the detector and features automated instrumentation control and data acquisition.

While complex systems of this type have allowed researchers to explore the spectroscopic properties of oral tissue in detail, the recent trend has been towards smaller, portable devices that are easy to use in the clinic and require minimal user adjustment during daily operation. These devices are often designed to measure only a few selected spectra whose diagnostic value has been previously established. This trend has been accelerated by the availability of inexpensive, high spectral brightness light-emitting diodes (LEDs), which are frequently used in place of laser sources or arc lamp/flashlamp sources and by the availability of high-performance miniature spectrometers and detectors. Figure 2c shows a clinical system reported by Amelink et al. for differential path length reflectance spectroscopy that exemplifies the trend towards simple, miniaturized devices that measure only selected spectra of interest [31].

A key component of most clinical spectroscopic instruments is the fiber optic probe, which transmits the excitation light to the tissue and returns the collected light to the detection system. A multitude of probe designs and configurations have been reported in the literature as reviewed by Utzinger [32]. The geometric arrangement of excitation and collection fibers can be used to maximize the desired spectral signal or interrogate the tissue in a specific manner (Fig. 3). Angled or side-looking probes are common [33]. Different depths in tissue may be interrogated through the use of different source–detector fiber separations, designs that incorporate miniature lenses, or differential path length configurations [31, 34–36]. The fiber optic probe is typically (though not always) designed to be placed in contact with the tissue at the measurement site. This implies that there should be some method for guiding the selection of sites to be measured with the spectroscopic probe. This may be either the clinician's judgment or some type of macroscopic imaging or scanning technique that can rapidly identify high-risk regions within the oral cavity [37].

Fig. 3 (continued) reflection (θ_{crit} = critical angle); (**g**) illumination and collection using the same fiber; (**h**) illumination and collection using adjacent fibers; (**i–j**) illumination and collection using adjacent fibers, with beveled fibers to improve collection efficiency; (**k**) hexagonal fiber configuration for submersion; (**l**) hexagonal fiber configuration for measurement of surfaces; (**m**) single excitation fiber and multiple collection fibers at different source–detector separations to sample different depths within tissue. Adapted with permission from Utzinger U and Richards-Kortum RR, *J Biomed Opt*. 2003;8(1):121–147

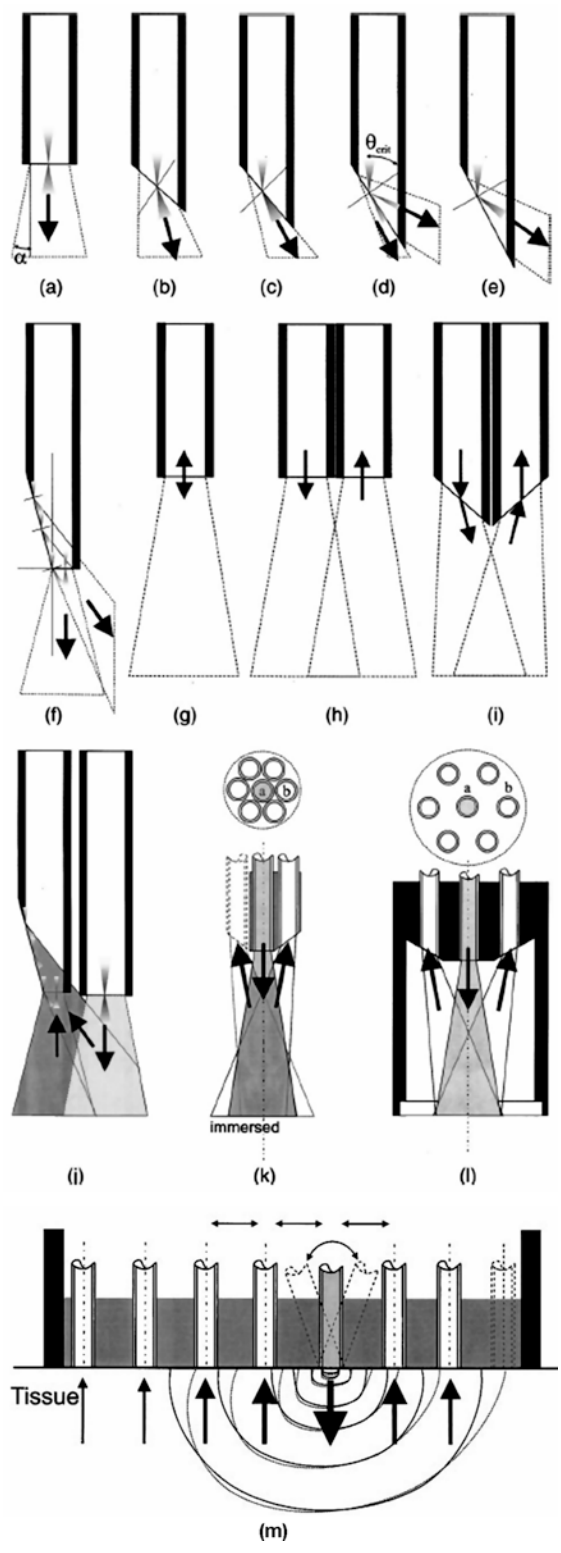

Fig. 3 Examples of fiber optic probe configurations. (**a**) The output of an optical fiber is described by the half angle α or the numerical aperture; (**b**–**c**) oblique polishing of the fiber tip deflects the output beam; (**d**–**f**) part or all of the output beam may be directed sideways through the use of reflective coatings or total internal

Analysis Methods

Analysis of clinical spectroscopic data from oral tissue has generally focused on two areas: (1) determination of biological properties of tissue, such as concentration and distribution of specific fluorophores and absorbers, based on the measured spectra; and (2) determination of the disease state of the tissue based on the measured spectra and/or biological properties calculated from the measured spectra. Diagnostic performance is evaluated by comparing spectroscopic results to a gold standard, such as histopathology, from the measured site.

Mathematical models of light propagation in tissue are typically used as the starting point for data analysis. These models are beyond the scope of this chapter and are only mentioned briefly here; extensive information is available in the literature [38–41]. The models describe tissue in terms of wavelength-dependent optical properties including absorption, scattering, anisotropy, reduced scattering, and refractive index [42]. These definitions typically require simplifying assumptions in which parameter values are assigned uniformly to certain regions or layers of tissue.

The most general approach to modeling light propagation in tissue involves the radiative transport equation (RTE), which describes the propagation of electromagnetic radiation through a medium in which absorption, scattering, and emission occur [43]. The RTE can be solved numerically or can be simplified by further approximations to obtain closed form solutions. The diffusion approximation, in which absorption is assumed to be minimal compared to scattering, is frequently used; but its applicability is limited, especially at short source–detector separations [44]. Higher-order solutions to the RTE such as the P_3 approximation may also be used [39]. An alternative approach is the use of Monte Carlo models, which simulate the propagation of large numbers (millions) of photons through computer-based virtual models of tissue, with the trajectory of each photon governed by probabilities for absorption, scattering, and emission events based on the local properties of the modeled tissue [45–47]. The Monte Carlo model output consists of the aggregate results from these millions of tracked photons.

Whatever particular modeling approach is selected, the model parameters are optimized and adjusted based on comparison of the model output to experimentally measured spectra. Once sufficient agreement is established between the model and measured data, further experimental measurements may be used to calculate tissue properties and biological parameters. Spectral features, calculated tissue properties, and/or calculated biological parameters are then used to predict the disease state of the tissue. Mathematical techniques such as principal component analysis may be used to reduce

the dimensionality of the data. Diagnostic prediction algorithms may involve classification techniques such as linear discriminant analysis, logistic regression, cluster analysis, neural networks, decision trees, and other methods [48–50].

Clinical Studies

Studies by Alfano et al. in animal tissue and nonoral human tissues established the potential for spectroscopic diagnosis of dysplasia and cancer [20, 21]. Kolli et al. performed early spectroscopic studies of oral lesions in vivo, measuring 31 patients with primary intraepithelial neoplasia or invasive squamous cell carcinoma of the oral cavity and pharynx using a Xenon flashlamp-based spectroscopy system [51]. Using a portable spectrofluorimeter with a nitrogen-pumped dye laser source, Dhingra et al. observed reduced autofluorescence intensity in neoplastic lesions compared to normal tissue in broad emission peaks centered at 450 nm (at 370 nm excitation) and 490 nm (at 410 nm excitation) [52]. In a study of 49 patients, Betz et al. similarly reported reduced autofluorescence emission intensity from neoplastic oral mucosa compared to normal tissue in the 500-nm wavelength region [53]. Interestingly, these measurements were performed in a noncontact configuration using an endoscope with a Xenon arc lamp, a CCD camera, and a spectrometer.

As successive clinical studies showed alterations in autofluorescence emission in diseased tissue relative to healthy tissue (typically reduced blue–green autofluorescence intensity, and sometimes increased red autofluorescence associated with porphyrins), researchers began to systematically explore the optimal excitation and emission wavelengths for detecting these disease-related spectroscopic changes. Heintzelman et al. identified optimal excitation wavelengths for detection of oral neoplasia as 350, 380, and 400 nm, paired with an emission wavelength of 472 nm [54]. They reported 90 % sensitivity and 88 % specificity in a training set of 20 subjects, and 100 % sensitivity and 98 % specificity in a validation set of 56 subjects, for distinguishing normal oral tissue from dysplasia and cancer. Figure 4 shows fluorescence excitation-emission matrices (EEMs) from cancerous and normal tissue measured in this study, collected using a Xenon arc lamp-based spectroscopy system. Van Staveren et al. reported the use of artificial neural network classification methods to distinguish abnormal from normal oral tissue with 86 % sensitivity and 100 % specificity in a study of 23 subjects, based on 420 nm excitation and 465–650 nm emission [48].

Autofluorescence spectra measured from tissue may be substantially affected by absorption of excitation and/or emission

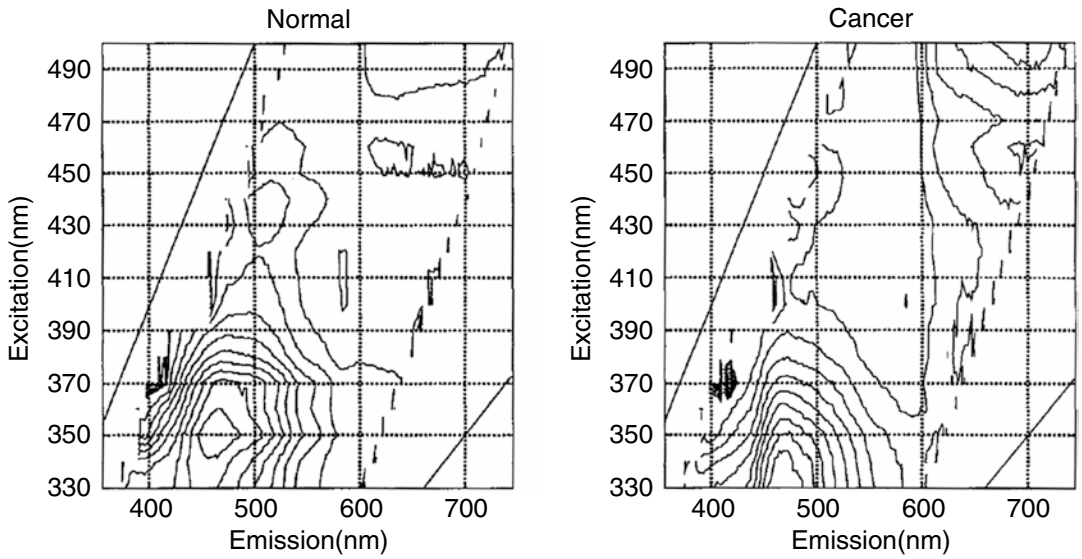

Fig. 4 Fluorescence excitation emission matrices (EEMs) from normal and cancerous oral tissue. *nm* nanometers. Reprinted with permission from Heintzelman DL, Utzinger U, Fuchs H, et al. *Photochem Photobiol*. 2000;72(1):103–113

light by oxy and deoxyhemoglobin present in the blood within intact tissue. Modeling and analysis of these effects are further complicated by the fact that blood is located within the vessels of varying diameter, rather than uniformly distributed throughout the tissue [55]. Müller et al. demonstrated the use of information from reflectance spectra to correct for the effects of hemoglobin absorption on fluorescence spectra, resulting in "intrinsic" fluorescence spectra [56] (Fig. 5). In the same study, the authors extracted biological parameters from the measured spectra (contributions to the intrinsic fluorescence spectra from NADH and collagen) and used them to classify tissue in binary decision plots [56] (Fig. 6). De Veld et al. also implemented a mathematical method for correcting autofluorescence spectra for the effects of blood absorption based on diffuse reflectance measurements [57]. In a study of 155 patients and 70 healthy volunteers, they reported excellent discrimination of cancer from healthy tissue [area under receiver operator characteristic curve (AUC) = 0.98] and successful discrimination of lesions from healthy mucosa (AUC = 0.90). However, they found that discrimination of benign lesions from dysplastic and malignant lesions was less successful (AUC = 0.77) [57].

In recent clinical studies, researchers have explored new measurement configurations, implemented probe designs that target the epithelial layer where early precancerous changes occur, examined the effects of different oral sites on spectral measurements,

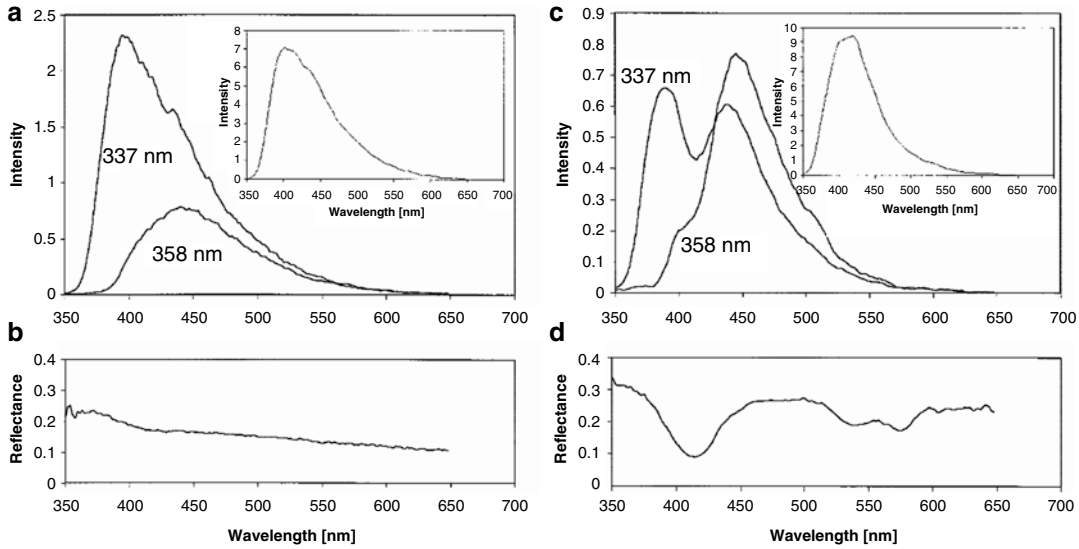

Fig. 5 Fluorescence spectra (**a**, **c**) measured at two oral sites, each excited at 337 nm and 358 nm, respectively, and corresponding reflectance spectra (**b**, **d**) at the same sites. Differences in fluorescence line shape between (**a**) and (**c**) are for the most part due to hemoglobin variations, which can also be observed in the corresponding reflectance spectra (**b**, **d**). The insets show the calculated 337-nm excited intrinsic fluorescence. *nm* nanometers. Reprinted with permission from Müller MG, Valdez TA, Georgakoudi I, et al. *Cancer*. 2003;97:1681–1692

and investigated the challenge of distinguishing benign lesions such as inflammation from dysplastic and cancerous lesions. Nieman et al. reported a study of 27 patients using oblique polarized reflectance spectroscopy [58]. Schwarz et al. measured 60 patients and 64 healthy volunteers using Xenon arc lamp-based spectroscopy system with a ball lens coupled fiber optic probe, which permits depth-sensitive targeting of epithelial or stromal regions [59] (Fig. 7). In this study, normal/benign lesions and mild dysplasia were distinguished from moderate/severe dysplasia and cancer with an AUC of 0.96 in the training set and 0.93 in the validation set. McGee et al. reported anatomy-based algorithms for spectroscopic diagnosis based on the properties of different anatomic sites within the oral cavity [60]. Amelink et al. developed a configuration for differential path length spectroscopy and used it to distinguish dysplastic from nondysplastic leukoplakias with an AUC of 0.87 in a study of 18 patients [31, 61].

Multimodal Diagnostics

In addition to point-probe spectroscopy, other noninvasive optical modalities for in vivo detection of oral dysplasia and cancer include macroscopic autofluorescence imaging and high-resolution

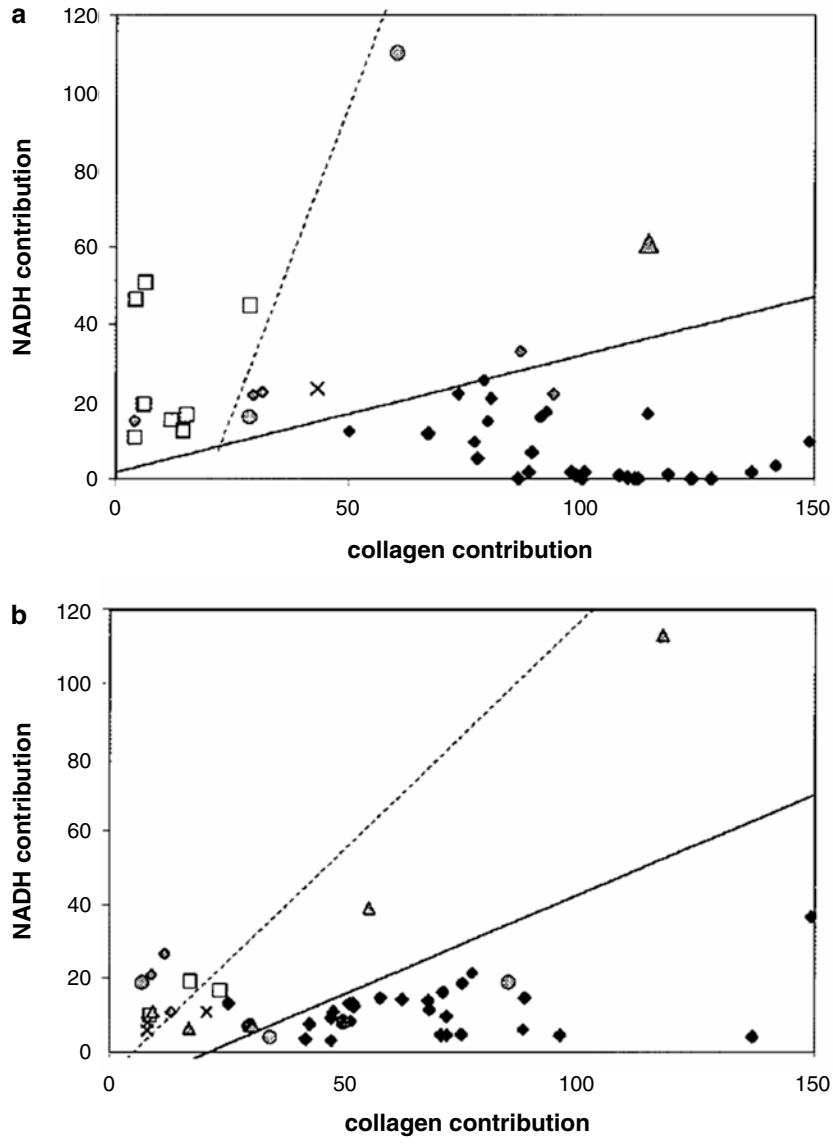

Fig. 6 Binary decision plots demonstrating the contributions of collagen and NADH to the intrinsic fluorescence tissue spectra at 337 nm and 358 nm excitation. (**a**) Nonkeratinized epithelium. (**b**) Keratinized epithelium. Note that the collagen contribution decreases and the NADH contribution increases with progression towards malignancy. The *solid line* separates normal from abnormal tissue and the *dotted line* separates dysplastic from cancerous tissue. *Darkly shaded* diamond: normal. *Darkly shaded* triangle: mild dysplasia. *Shaded circle*: moderate dysplasia. *Lightly shaded* diamond: severe dysplasia. *Open square*: cancer. *Solid circle*: inflammation. X: hyperkeratosis. *NADH* nicotinamide adenine dinucleotide, *nm* nanometers. Reprinted with permission from Müller MG, Valdez TA, Georgakoudi I, et al. *Cancer*. 2003;97:1681–1692

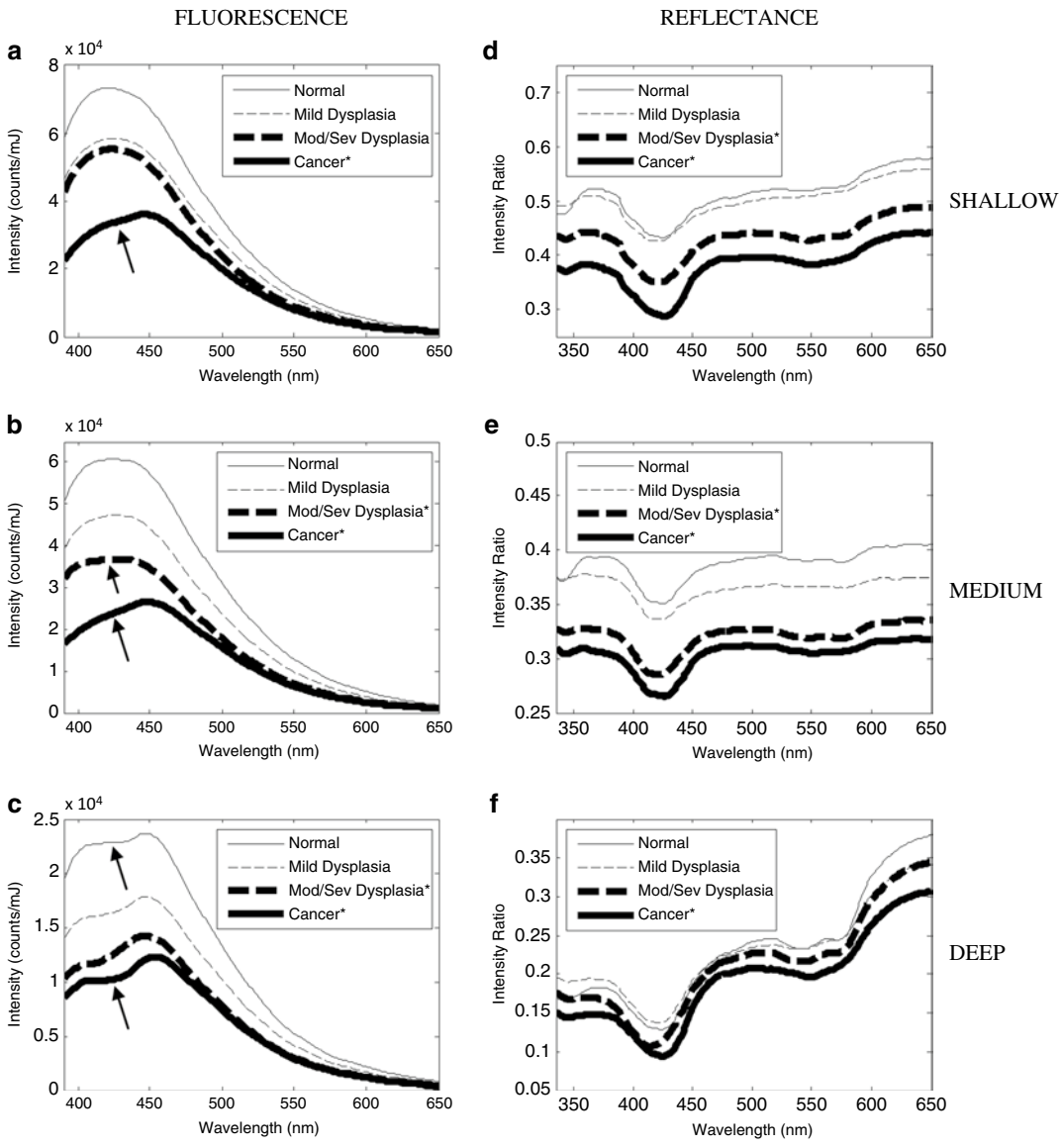

Fig. 7 Average spectra of nonkeratinized oral tissue by diagnosis, illustrating differences in data obtained at different depths. *Left column*: Fluorescence spectra at 350 nm excitation; *arrows* indicate absorption of fluorescent light by hemoglobin. *Right column*: Reflectance spectra with *white* light illumination. *Top*, *middle*, and *bottom*: Shallow, medium, and deep target depths (epithelium, basal epithelium/shallow stroma, and stroma, respectively). An *asterisk* (*) next to a diagnostic category indicates a statistically significant difference with respect to normal tissue. *Mod/Sev* moderate/severe, *mJ* millijoule, *nm* nanometers. Reprinted with permission from Schwarz RA, Gao W, Weber CR, et al. *Cancer*. 2009;115:1669–1679

imaging [62, 63]. These methods operate on different spatial scales from spectroscopy and are sensitive to different tissue parameters. Macroscopic autofluorescence imaging is sensitive to loss of autofluorescence in the stroma; spectroscopy is sensitive to metabolic changes, architectural changes, and angiogenesis; and high-resolution imaging is sensitive to nuclear morphology in the superficial epithelium. The combination of fluorescence and reflectance spectroscopy with optical imaging modalities offers certain advantages. Macroscopic autofluorescence imaging can be used to quickly identify high-risk regions within the oral cavity and guide the placement of the spectroscopic probe. Data from autofluorescence imaging, spectroscopy, and/or high-resolution imaging may be combined to provide a more complete analysis of the tissue and improved diagnostic specificity. Two-step diagnostic algorithms may be constructed based on different modalities, with the threshold in the first step set for high sensitivity and the threshold in the second step set for high specificity.

There are several commercially available macroscopic autofluorescence imaging devices that may be used in combination with spectroscopy. One such device is the VELscope® (LED Dental Ltd., Atlanta, Georgia), which is a handheld instrument that allows direct visualization of tissue fluorescence [64, 65]. An independent study suggests that it has a high sensitivity for detecting oral mucosal disorders, but a low specificity for dysplasia [66]. The VELscope may be used to guide placement of the spectroscopic probe, thus taking advantage of the VELscope's sensitivity while potentially improving diagnostic specificity.

An early example of the multimodal combination of imaging and spectroscopy is the work of Onizawa et al., who combined fluorescence film photography with measurements of autofluorescence using a chroma meter [67]. A second example is the previously mentioned study by Betz et al., in which a beamsplitter was used to direct a small portion of the light from the center of the endoscopic fluorescence image to an optical multichannel analyzer for spectral analysis [53]. More recently, Bedard et al. reported a pilot clinical study using a hyperspectral imaging device called a snapshot spectral imaging spectrometer [68]. This device collects image data with a complete spectrum associated with each pixel in the image (Fig. 8).

Discussion

A large and growing body of research indicates that fluorescence and reflectance spectroscopy can be useful tools to aid clinicians in detecting oral dysplasia and cancer. Optical spectroscopy has certain advantages. It is a straightforward method to implement in a clinical setting and clinical devices can be made small and portable.

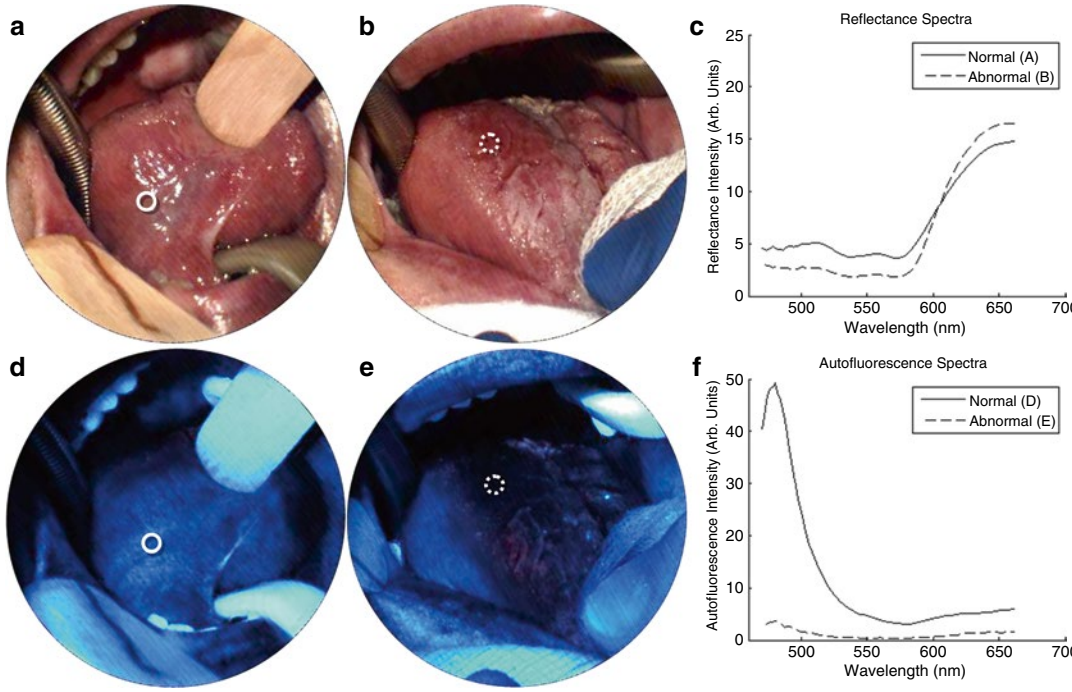

Fig. 8 Hyperspectral imaging using the snapshot spectral imaging spectrometer. (**a**, **d**) *Right ventral tongue* (clinical description: normal) in reflectance and autofluorescence modes, respectively. A biopsy (*solid circle*) indicated normal epithelium. (**b**, **e**) *Right dorsal tongue* (clinical description: erythroplakia) in reflectance and autofluorescence modes, respectively. A biopsy (*dotted circle*) indicated squamous cell carcinoma. Reflectance spectra (C) display characteristic oxyhemoglobin peaks. Autofluorescence images and spectra (F) show loss of *blue-green* autofluorescence at the abnormal site. Reprinted with permission from Bedard N, Schwarz RA, Hu A, et al. *Biomed Opt Express*. 2013;4(6):938–949

A variety of spectroscopic techniques, illumination and collection wavelengths, and probe designs can be tailored for specific applications. Spectral measurements provide quantitative data that can be rapidly analyzed at the point of care to provide information about tissue composition, tissue structure, and disease status. Spectral data from point probe measurements can readily be analyzed in an objective, quantitative manner without some of the concerns involved in quantitative image analysis, such as how to select appropriate regions of interest within an image. It is relatively easy to create a set of physical reference standards that can be measured frequently to monitor system performance over time during clinical studies [69].

Spectroscopy does, however, have a number of important limitations for in vivo screening and diagnosis, as summarized in a useful review by de Veld et al. [70]. In order to relate the measured spectra to biological characteristics of tissue it is necessary to

account for the complex interplay of autofluorescence, scattering, absorption, and tissue architecture. The mathematical models used for the analysis often require significant simplifying assumptions or prior knowledge regarding local tissue composition and structure [71]. Variations are often observed in spectra measured from healthy tissue in different patients or from different oral sites. Point-probe spectroscopy only provides information about the sites selected for measurement; it can therefore be subject to sampling error and it cannot easily be used to screen large regions of the oral mucosa. The method used to guide probe placement, whether clinical judgment or some other technique, must be considered carefully. Accurate spatial correlation of measured sites with biopsy specimens or locations on surgical specimens is essential and may be more challenging than it first appears. While evidence in the literature shows that spectroscopy can accurately distinguish healthy tissue from dysplasia and cancer, the presence of benign lesions can complicate diagnostic classification. Finally, spectral data may not have the direct visual appeal of image-based techniques that display macroscopic or microscopic views of tissue.

The development of commercial spectroscopic devices for diagnosis of oral neoplasia has lagged behind the development of commercial imaging devices such as the VELscope. Even so, the potential for clinical use of spectroscopy remains high. It is most likely to be clinically implemented in combination with macroscopic imaging methods to guide probe placement, or in multimodal devices such as the snapshot spectral imaging spectrometer [68]. If spectroscopy can consistently help reduce the false positive rate associated with autofluorescence imaging, it will be a valuable diagnostic tool. Rapid, noninvasive optical techniques including spectroscopy are particularly well suited for use in low-resource settings, where laboratory facilities and expertise for conventional diagnosis may not be available [72].

In the future, the role of clinical spectroscopy and imaging may be transformed as molecular specific contrast agents for the identification of dysplasia and cancer become available for in vivo clinical use. The combination of molecular specific labeling with high spectral- and spatial-resolution optical methods could open up new opportunities for screening and diagnosis of dysplasia and cancer, as well as assessment of surgical margins. In our own research with resected tissue specimens labeled ex vivo using molecular specific contrast agents, we have found spectroscopy to be a useful tool to determine the penetration and localization of the contrast agent within the tissue. With the rapid growth in molecular imaging and the increasing availability of molecular probes for targeting specific biomarkers, spectroscopic measurement techniques for interrogating these probes will continue to be of interest.

References

1. Ferlay J, Shin HR, Bray F, Forman D, Mathers C, Parkin DM. Estimates of worldwide burden of cancer in 2008: GLOBOCAN 2008. Int J Cancer. 2010;127:2893–917.
2. Jemal A, Siegel R, Xu J, Ward E. Cancer statistics, 2010. CA Cancer J Clin. 2010;60:277–300.
3. Kalavrezos N, Bhandari R. Current trends and future perspectives in the surgical management of oral cancer. Oral Oncol. 2010;46:429–32.
4. Ow TJ, Myers JN. Current management of advanced resectable oral cavity squamous cell carcinoma. Clin Exp Otorhinolaryngol. 2011;4(1):1–10.
5. Rapidis AD, Gullane P, Langdon JD, Lefebvre JL, Scully C, Shah JP. Major advances in the knowledge and understanding of the epidemiology, aetiopathogenesis, diagnosis, management and prognosis of oral cancer. Oral Oncol. 2009;45:299–300.
6. Petersen PE. Oral cancer prevention and control—the approach of the World Health Organization. Oral Oncol. 2009;45:454–60.
7. Lingen MW, Kalmar JR, Karrison T, Speight PM. Critical evaluation of diagnostic aids for the detection of oral cancer. Oral Oncol. 2008;44:10–22.
8. Fedele S. Diagnostic aids in the screening of oral cancer. Head Neck Oncol. 2009;1:5.
9. Ho MW, Risk JM, Woolgar JA, et al. The clinical determinants of malignant transformation in oral epithelial dysplasia. Oral Oncol. 2012;48:969–76.
10. Eckardt A, Barth EL, Kokemueller H, Wegener G. Recurrent carcinoma of the head and neck: treatment strategies and survival analysis in a 20-year period. Oral Oncol. 2004;40:427–32.
11. Richards-Kortum R, Sevick-Muraca E. Quantitative optical spectroscopy for tissue diagnosis. Annu Rev Phys Chem. 1996;47:555–606.
12. Fryen A, Glanz H, Lohmann W, Dreyer T, Bohle RM. Significance of autofluorescence for the optical demarcation of field cancerisation in the upper aerodigestive tract. Acta Otolaryngol. 1997;117:316–9.
13. Takatani S, Graham MD. Theoretical analysis of diffuse reflectance from a two-layer tissue model. IEEE Trans Biomed Eng. 1979;26(12):656–64.
14. Amelink A, Christiaanse T, Sterenborg HJCM. Effect of hemoglobin extinction spectra on optical spectroscopic measurements of blood oxygen saturation. Opt Lett. 2009;34(10):1525–7.
15. Mourant JR, Canpolat M, Brocker C, et al. Light scattering from cells: the contribution of the nucleus and the effects of proliferative status. J Biomed Opt. 2000;5(2):131–7.
16. Backman V, Gopal V, Kalashnikov M, et al. Measuring cellular structure at submicrometer scale with light scattering spectroscopy. IEEE J Sel Top Quantum Electron. 2001;7(6):887–93.
17. Policard A. Etude sur les aspects offerts par des tumeurs expérimentales examinées à la lumière de Wood. C R Soc Biol (Paris). 1924;91:1423–4.
18. Chance B, Thorell B. Localization and kinetics of reduced pyridine nucleotide in living cells by microfluorometry. J Biol Chem. 1959;234:3044–50.
19. Chance B, Cohen P, Jobsis F, Schoener B. Intracellular oxidation-reduction states in vivo. Science. 1962;137(3529):499–508.
20. Alfano RR, Tata DB, Cordero J, Tomashefsky P, Longo FW, Alfano MA. Laser induced fluorescence spectroscopy from native cancerous and normal tissue. IEEE J Quantum Electron. 1984;20(12):1507–11.
21. Alfano RR, Tang GC, Pradhan A, Lam W, Choy DSJ, Opher E. Fluorescence spectra from cancerous and normal human breast and lung tissues. IEEE J Quantum Electron. 1987;23(10):1806–11.
22. Bigio IJ, Bown SG. Spectroscopic sensing of cancer and cancer therapy. Cancer Biol Ther. 2004;3(3):259–67.
23. Mahadevan-Jansen A, Richards-Kortum R. Raman spectroscopy for the detection of cancers and precancers. J Biomed Opt. 1996;1(1):31–70.
24. Marcu L. Fluorescence lifetime techniques in medical applications. Ann Biomed Eng. 2012;40(2):304–31.
25. Gillenwater A, Jacob R, Richards-Kortum R. Fluorescence spectroscopy: a technique with potential to improve the early detection of aerodigestive tract neoplasia. Head Neck. 1998;20(6):556–62.
26. Inaguma M, Hashimoto K. Porphyrin-like fluorescence in oral cancer. Cancer. 1999;86:2201–11.
27. Pavlova I, Williams M, El-Naggar A, Richards-Kortum R, Gillenwater A. Understanding the biological basis of autofluorescence imaging for oral cancer detection: high-resolution fluorescence microscopy in viable tissue. Clin Cancer Res. 2008;14(8):2396–404.
28. Prahl SA (2013) Optical absorption of hemoglobin. Available at: http://omlc.ogi.edu/spectra/hemoglobin. Accessibility verified 12 Dec 2013.

29. Zheng W, Li D, Zeng Y, Luo Y, Qu JY. Two-photon excited hemoglobin fluorescence. Biomed Opt Express. 2010;2(1):71–9.
30. Tunnell JW, Desjardins AE, Galindo L, et al. Instrumentation for multi-modal spectroscopic diagnosis of epithelial dysplasia. Technol Cancer Res Treat. 2003;2(6):505–14.
31. Amelink A, Kaspers OP, Sterenborg HJCM, van der Wal JE, Roodenburg JLN, Witjes MJH. Non-invasive measurement of the morphology and physiology of oral mucosa by use of optical spectroscopy. Oral Oncol. 2008;44: 65–71.
32. Utzinger U, Richards-Kortum RR. Fiber optic probes for biomedical optical spectroscopy. J Biomed Opt. 2003;8(1):121–47.
33. Baran TM, Fenn MC, Foster TH. Determination of optical properties by interstitial white light spectroscopy using a custom fiber optic probe. J Biomed Opt. 2013; 18(10):107007.
34. Pfefer TJ, Schomacker KT, Ediger MN, Nishioka NS. Multiple-fiber probe design for fluorescence spectroscopy in tissue. Appl Opt. 2002;41(22):4712–21.
35. Pfefer TJ, Agrawal A, Drezek RA. Oblique-incidence illumination and collection for depth-selective fluorescence spectroscopy. J Biomed Opt. 2005;10(4):044016.
36. Schwarz RA, Gao W, Daye D, Williams MD, Richards-Kortum R, Gillenwater AM. Autofluorescence and diffuse reflectance spectroscopy of oral epithelial tissue using a depth-sensitive fiber-optic probe. Appl Opt. 2008; 47(6):825–34.
37. Roblyer D, Kurachi C, Stepanek V, et al. Objective detection and delineation of oral neoplasia using autofluorescence imaging. Cancer Prev Res (Phila). 2009;2(5):423–31.
38. Hielscher AH, Kim HK, Klose AD. Forward models of light transport in biological tissue. In: Boas DA, Pitris C, Ramanujam N, editors. Handbook of biomedical optics. Boca Raton, FL: CRC Press; 2011. p. 319–36.
39. Hull EL, Foster TH. Steady-state reflectance spectroscopy in the P_3 approximation. J Opt Soc Am A. 2001;18(3):584–99.
40. Jacques SL, Pogue BW. Tutorial on diffuse light transport. J Biomed Opt. 2008;13(4): 041302.
41. Patterson MS, Chance B, Wilson BC. Time resolved reflectance and transmittance for the non-invasive measurement of tissue optical properties. Appl Opt. 1989;28(12):2331–6.
42. Jacques SL. Optical properties of biological tissues: a review. Phys Med Biol. 2013;58:R37–61.
43. Arridge SR. Optical tomography in medical imaging. Inverse Prob. 1999;15:R41–93.
44. Hielscher AH, Alcouffe RE, Barbour RL. Comparison of finite-difference transport and diffusion calculations for photon migration in homogeneous and heterogeneous tissues. Phys Med Biol. 1998;43:1285–302.
45. Flock ST, Patterson MS, Wilson BC, Wyman DR. Monte Carlo modeling of light propagation in highly scattering tissues—I: model predictions and comparison with diffusion theory. IEEE Trans Biomed Eng. 1989;36(12): 1162–8.
46. Zhu C, Liu Q. Review of Monte Carlo modeling of light transport in tissues. J Biomed Opt. 2013;18(5):050902.
47. Pavlova I, Weber CR, Schwarz RA, Williams M, El-Naggar A, Gillenwater A, Richards-Kortum R. Monte Carlo model to describe depth selective fluorescence spectra of epithelial tissue: applications for diagnosis of oral precancer. J Biomed Opt. 2008;13(6):064012.
48. van Staveren HJ, van Veen RLP, Speelman OC, Witjes MJH, Star WM, Roodenburg JLN. Classification of clinical autofluorescence spectra of oral leukoplakia using an artificial neural network: a pilot study. Oral Oncol. 2000;36: 286–93.
49. de Veld DCG, Skurichina M, Witjes MJH, Duin RPW, Sterenborg HJCM, Roodenburg JLN. Clinical study for classification of benign, dysplastic, and malignant oral lesions using autofluorescence spectroscopy. J Biomed Opt. 2004;9(5):940–50.
50. Majumder SK, Gupta A, Gupta S, Ghosh N, Gupta PK. Multi-class classification algorithm for optical diagnosis of oral cancer. J Photochem Photobiol B. 2006;85:109–17.
51. Kolli VR, Savage HE, Yao TJ, Schantz SP. Native cellular fluorescence of neoplastic upper aerodigestive mucosa. Arch Otolaryngol Head Neck Surg. 1995;121(11):1287–92.
52. Dhingra JK, Perrault DF, McMillan K, et al. Early diagnosis of upper aerodigestive tract cancer by autofluorescence. Arch Otolaryngol Head Neck Surg. 1996;122(11):1181–6.
53. Betz CS, Mehlmann M, Rick K, et al. Autofluorescence imaging and spectroscopy of normal and malignant mucosa in patients with head and neck cancer. Lasers Surg Med. 1999;25:323–34.
54. Heintzelman DL, Utzinger U, Fuchs H, et al. Optimal excitation wavelengths for in vivo detection of oral neoplasia using fluorescence spectroscopy. Photochem Photobiol. 2000; 72(1):103–13.

55. Lau C, Šćepanović O, Mirkovic J, et al. Re-evaluation of model-based light-scattering spectroscopy for tissue spectroscopy. J Biomed Opt. 2009;14(2):024031.
56. Müller MG, Valdez TA, Georgakoudi I, et al. Spectroscopic detection and evaluation of morphologic and biochemical changes in early human oral carcinoma. Cancer. 2003;97:1681–92.
57. de Veld DCG, Skurichina M, Witjes MJH, Duin RPW, Sterenborg HJCM, Roodenburg JLN. Autofluorescence and diffuse reflectance spectroscopy for oral oncology. Lasers Surg Med. 2005;36:356–64.
58. Nieman LT, Kan CW, Gillenwater A, Markey MK, Sokolov K. Probing local tissue changes in the oral cavity for early detection of cancer using oblique polarized reflectance spectroscopy: a pilot clinical trial. J Biomed Opt. 2008;13(2):024011.
59. Schwarz RA, Gao W, Weber CR, et al. Noninvasive evaluation of oral lesions using depth-sensitive optical spectroscopy. Cancer. 2009;115:1669–79.
60. McGee S, Mardirossian V, Elackattu A, et al. Anatomy-based algorithms for detecting oral cancer using reflectance and fluorescence spectroscopy. Ann Otol Rhinol Laryngol. 2009; 118(11):817–26.
61. Amelink A, Sterenborg HJCM, Roodenburg JLN, Witjes MJH. Non-invasive measurement of the microvascular properties of non-dysplastic and dysplastic oral leukoplakias by use of optical spectroscopy. Oral Oncol. 2011;47: 1165–70.
62. Roblyer D, Richards-Kortum R, Sokolov K, et al. Multispectral optical imaging device for in vivo detection of oral neoplasia. J Biomed Opt. 2008;13(2):024019.
63. Pierce M, Yu D, Richards-Kortum R. High-resolution fiber-optic microendoscopy for in situ cellular imaging. J Vis Exp. 2011;47:e2306. doi:10.3791/2306.
64. Lane PM, Gilhuly T, Whitehead P, et al. Simple device for the direct visualization of oral-cavity tissue fluorescence. J Biomed Opt. 2006; 11(2):024006.
65. Poh CF, Ng SP, Williams PM, et al. Direct fluorescence visualization of clinically occult high-risk oral premalignant disease using a simple hand-held device. Head Neck. 2007; 29:71–6.
66. Awan KH, Morgan PR, Warnakulasuriya S. Evaluation of an autofluorescence based imaging system (VELscope™) in the detection of oral potentially malignant disorders and benign keratoses. Oral Oncol. 2011;47:274–7.
67. Onizawa K, Yoshida H, Saginoya H. Chromatic analysis of autofluorescence emitted from squamous cell carcinomas arising in the oral cavity: a preliminary study. Int J Oral Maxillofac Surg. 2000;29:42–6.
68. Bedard N, Schwarz RA, Hu A, et al. Multimodal snapshot spectral imaging for oral cancer diagnostics: a pilot study. Biomed Opt Express. 2013;4(6):938–49.
69. Marín NM, MacKinnon N, MacAulay C, et al. Calibration standards for multicenter clinical trials of fluorescence spectroscopy for in vivo diagnosis. J Biomed Opt. 2006;11(1): 014010.
70. de Veld DCG, Witjes MJH, Sterenborg HJCM, Roodenburg JLN. The status of in vivo autofluorescence spectroscopy and imaging for oral oncology. Oral Oncol. 2005;41:117–31.
71. Pavlova I, Weber CR, Schwarz RA, Williams MD, Gillenwater AM, Richards-Kortum R. Fluorescence spectroscopy of oral tissue: Monte Carlo modeling with site-specific tissue properties. J Biomed Opt. 2009;14(1): 014009.
72. Gray LV, Schwarz RA, Richards-Kortum R. Imaging as a tool for global cancer control. Comput Med Imaging Graph. 2013;37: 195–6.